Supplementary Information

Four New Luminescent Metal-Organic Frameworks as Multifunctional Sensors for Detecting Fe^{3+}, $Cr_2O_7^{2-}$ and Nitromethane

Fa-Yuan Ge,[†] Guo-Hao Sun,[†] Lei Meng,[‡,*] Shuang-Shuang Ren[†] and He-Gen Zheng[†,*]

[†]*State Key Laboratory of Coordination Chemistry, School of Chemistry and Chemical Engineering, Collaborative Innovation Center of Advanced Microstructures, Nanjing University, Nanjing 210023, P. R. China.*

[‡]*College of Science, Henan Agricultural University, Zhengzhou, 450002 P. R. China.*

E-mail: zhenghg@nju.edu.cn; Fax: (+86)-25-89682309

E-mail: xleimeng@163.com.

Figure **S1**. IR spectrum of the L ligand.

Figure **S2**. IR spectrum of MOF **1**.

Figure **S3**. IR spectrum of MOF **2**.

Figure **S4**. IR spectrum of MOF **3**.

Figure **S5**. IR spectrum of MOF **4**.

Figure **S6**. The PXRD patterns of **1** before and after immersed in Fe^{3+}, $Cr_2O_7^{2-}$ and nitromethane for 3 days.

Figure **S7**. The PXRD patterns of **2** before and after immersed in Fe^{3+}, $Cr_2O_7^{2-}$ and nitromethane for 3 days.

Figure **S8**. The PXRD patterns of **3** before and after immersed in Fe^{3+}, $Cr_2O_7^{2-}$ and nitromethane for 3 days.

Figure **S9**. The PXRD patterns of **4** before and after immersed in Fe^{3+}, $Cr_2O_7^{2-}$ and nitromethane for 3 days.

Figure **S10**. The TGA diagram of MOF **1**.

Figure **S11**. The TGA diagram of MOF **2**.

Figure **S12**. The TGA diagram of MOF **3**.

Figure **S13**. The TGA diagram of MOF **4**.

Figure **S14**. Liquid UV/vis spectra of different metal cations in aqueous solutions.

Figure **S15**. Liquid UV/vis spectra of different anions in aqueous solutions.

Figure **S16**. Solid state UV/vis spectra of MOFs **1-4**.

Table **S1**. Crystal date for complexes **1-4**.

Table **S2**. Selected bond lengths and angles for MOFs **1-4**.

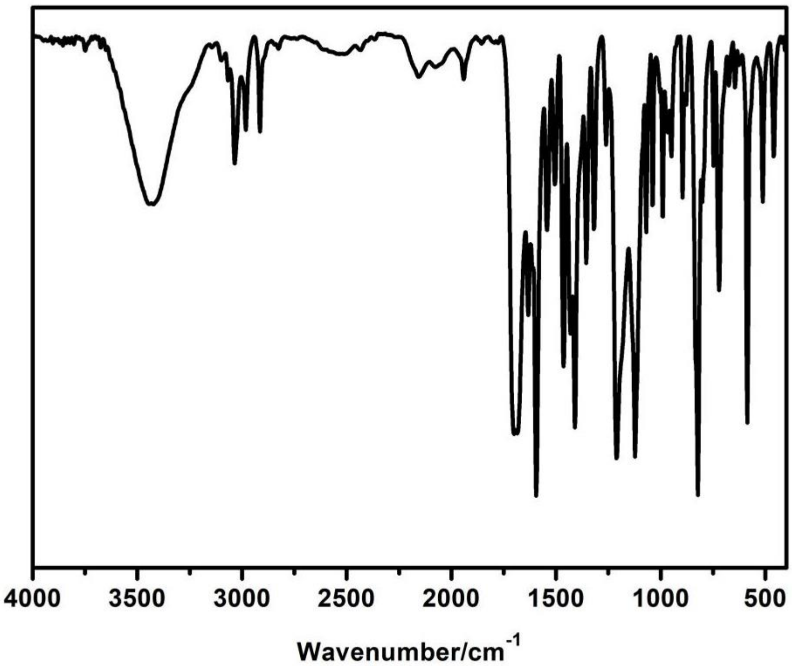

Figure **S1** IR spectrum of the L ligand**.**

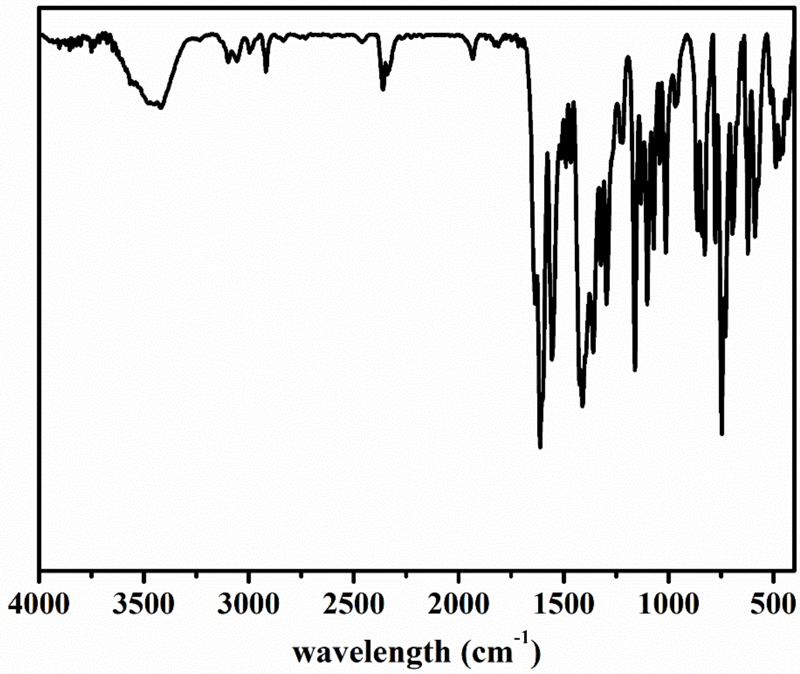

Figure **S2** IR spectrumof MOF **1**.

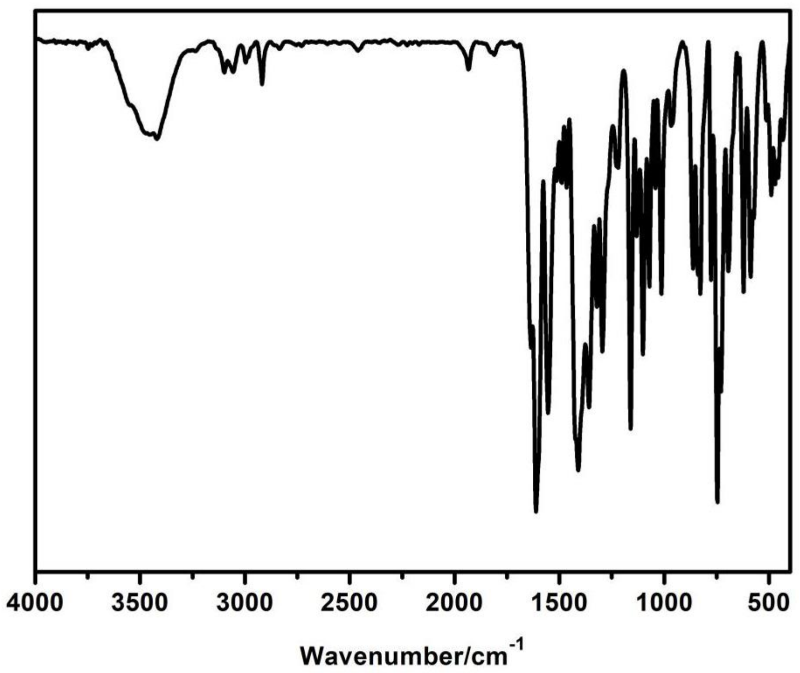

Figure **S3** IR spectrum of MOF **2**.

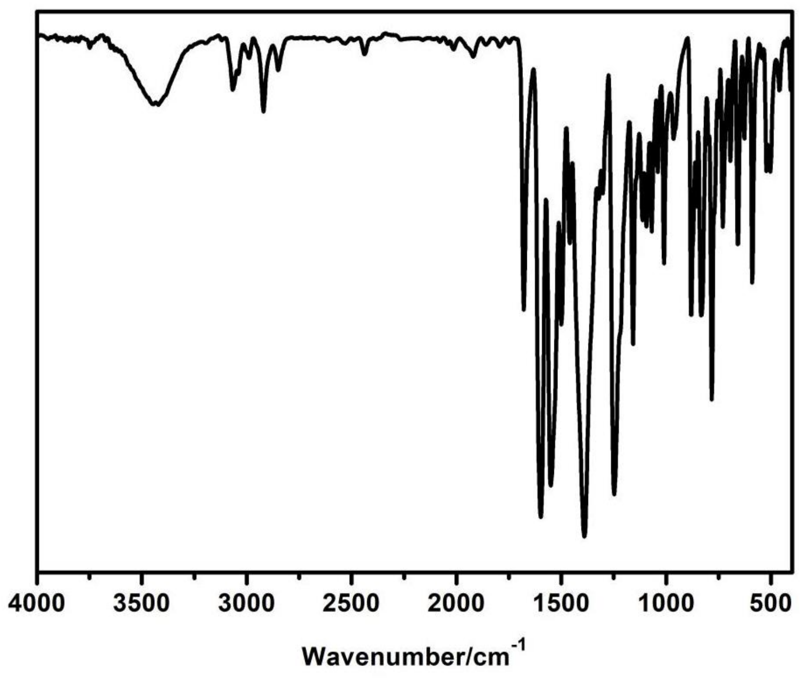

Figure **S4** IR spectrum of MOF **3**.

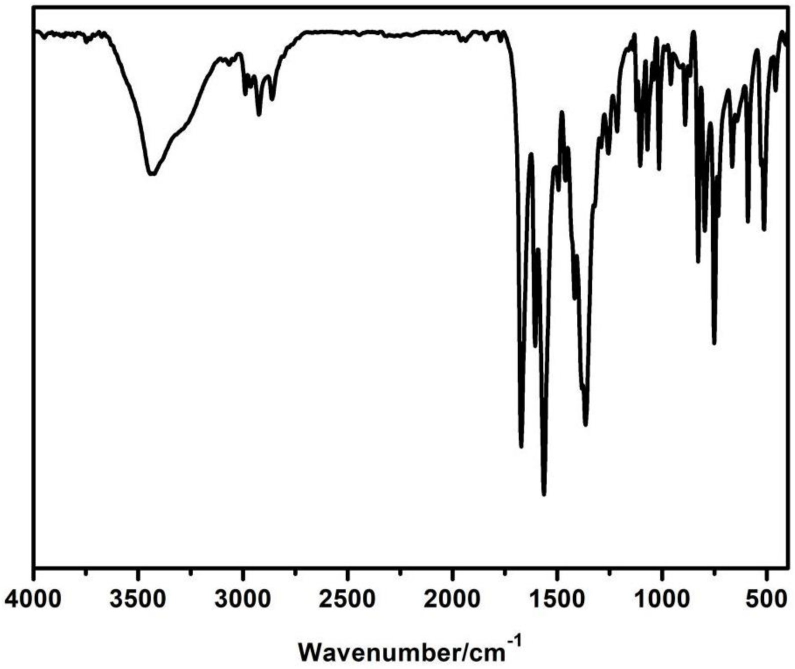

Figure **S5** IR spectrum of MOF **4**.

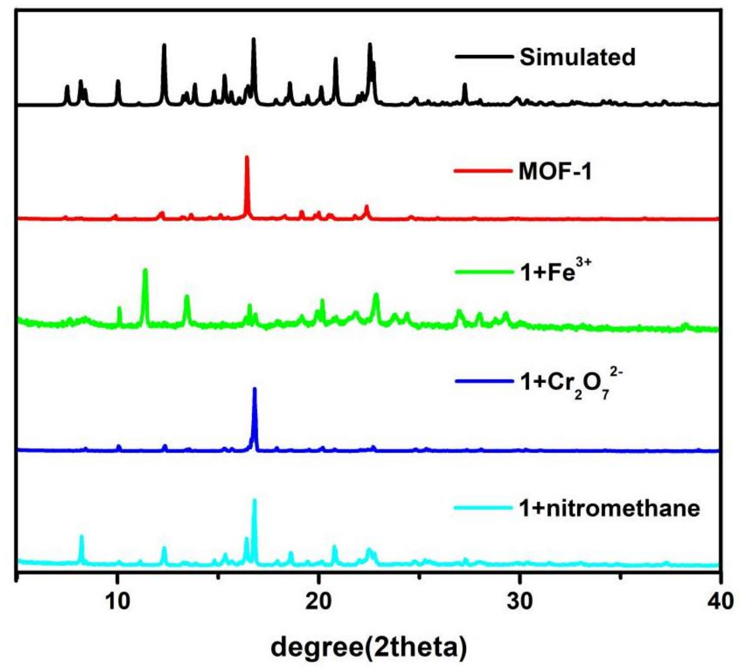

Figure **S6** The PXRD patterns of **1** before and after immersed in Fe^{3+}, $Cr_2O_7^{2-}$ and nitromethane for 3 days.

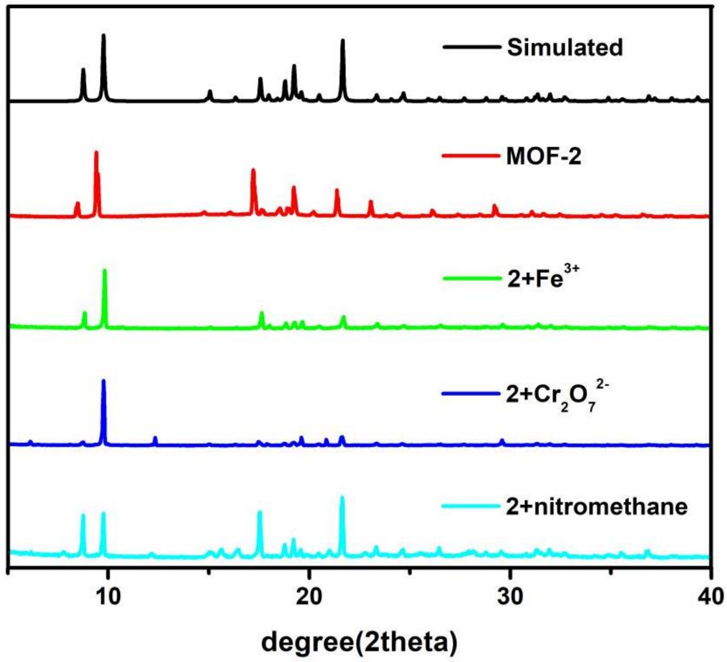

Figure **S7** The PXRD patterns of **2** before and after immersed in Fe^{3+}, $Cr_2O_7^{2-}$ and nitromethane for 3 days.

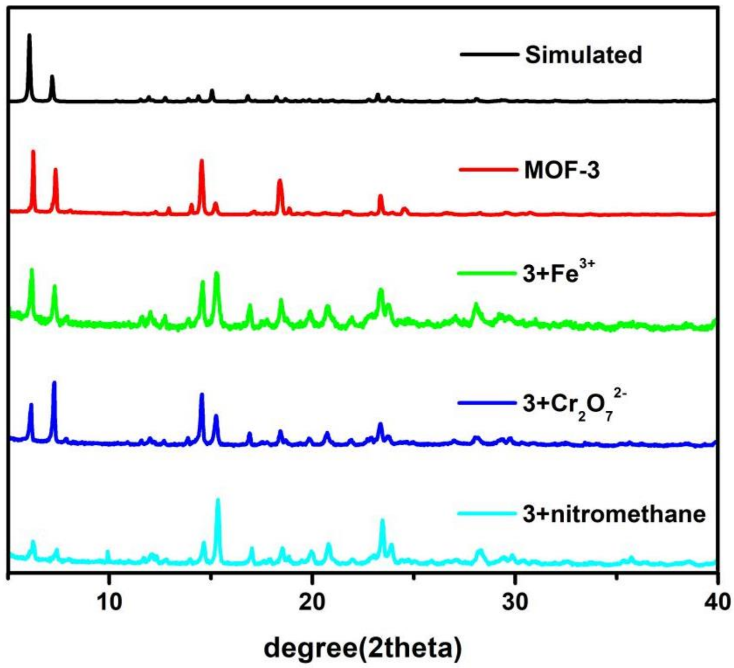

Figure **S8** The PXRD patterns of **3** before and after immersed in Fe^{3+}, $Cr_2O_7^{2-}$ and nitromethane for 3 days.

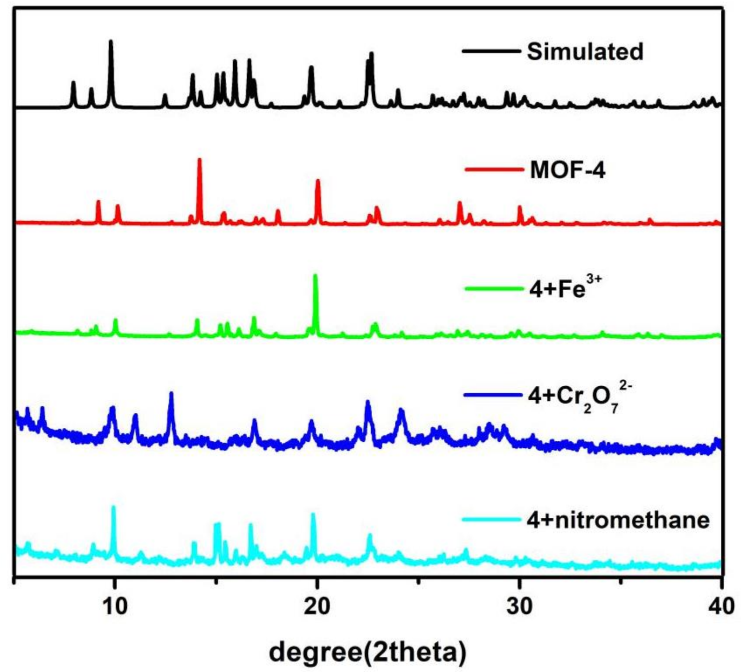

Figure **S9** The PXRD patterns of **4** before and after immersed in Fe^{3+}, $Cr_2O_7^{2-}$ and nitromethane for 3 days.

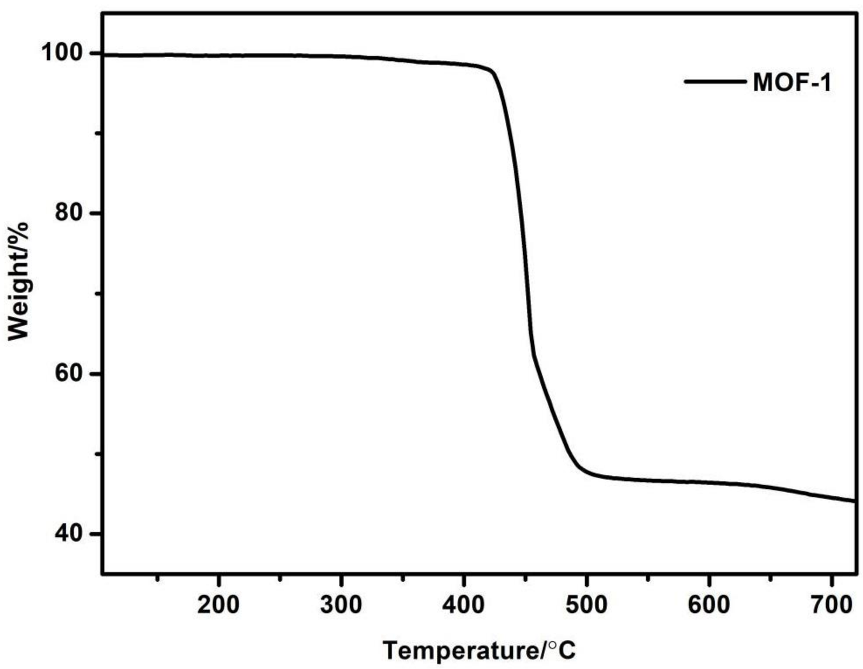

Figure **S10** The TGA diagram of MOF **1**.

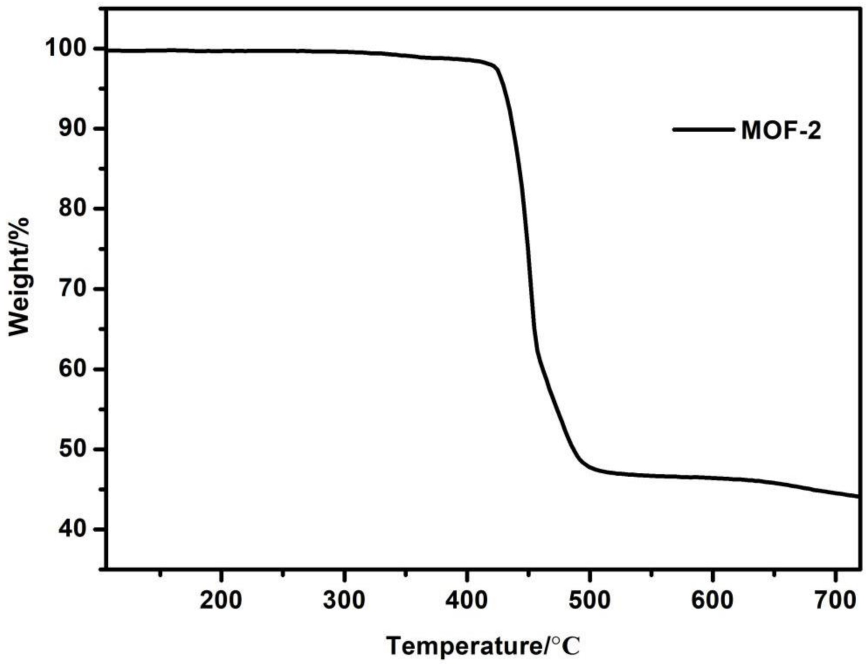

Figure **S11** The TGA diagram of MOF **2**.

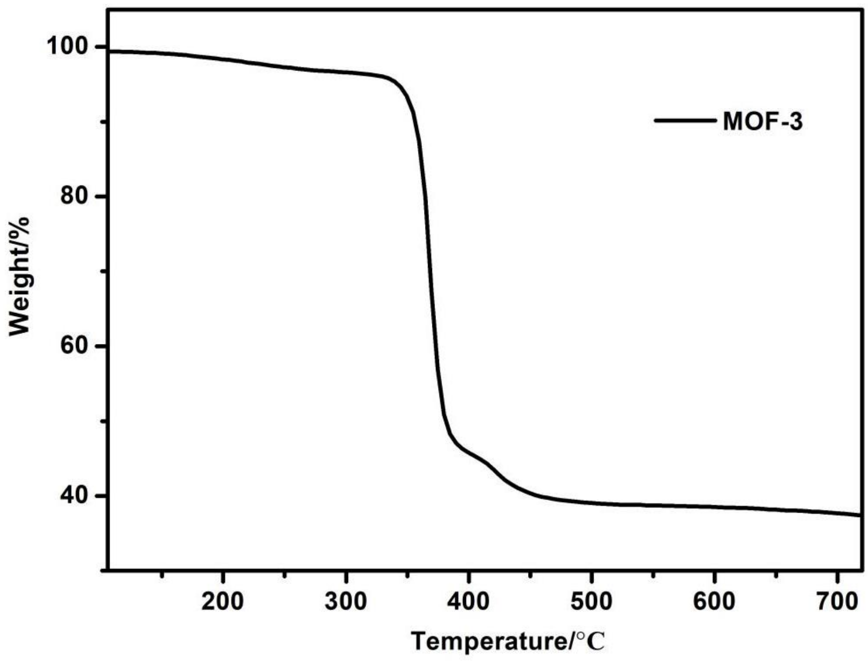

Figure **S12** The TGA diagram of MOF **3**.

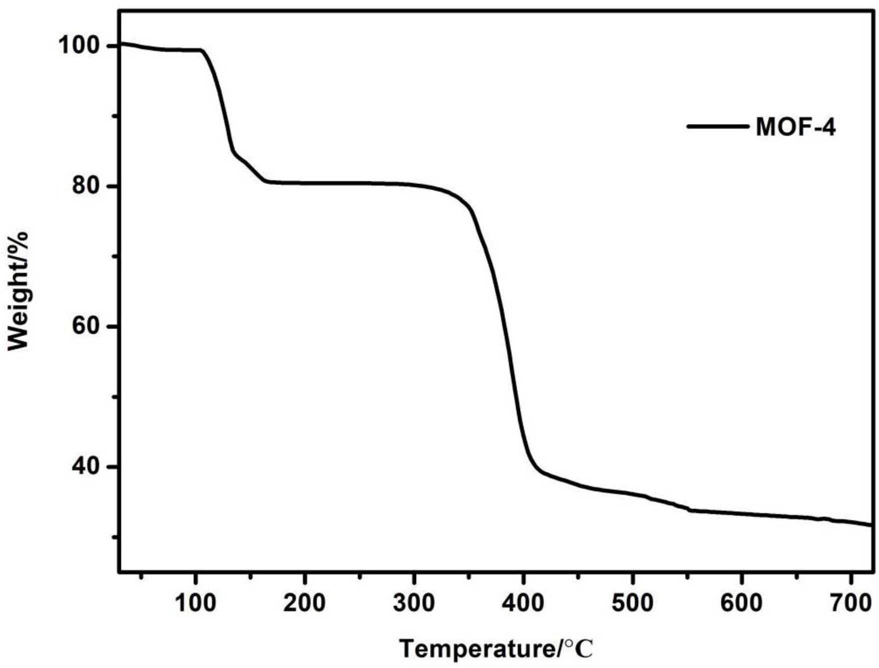

Figure **S13** The TGA diagram of MOF **4**.

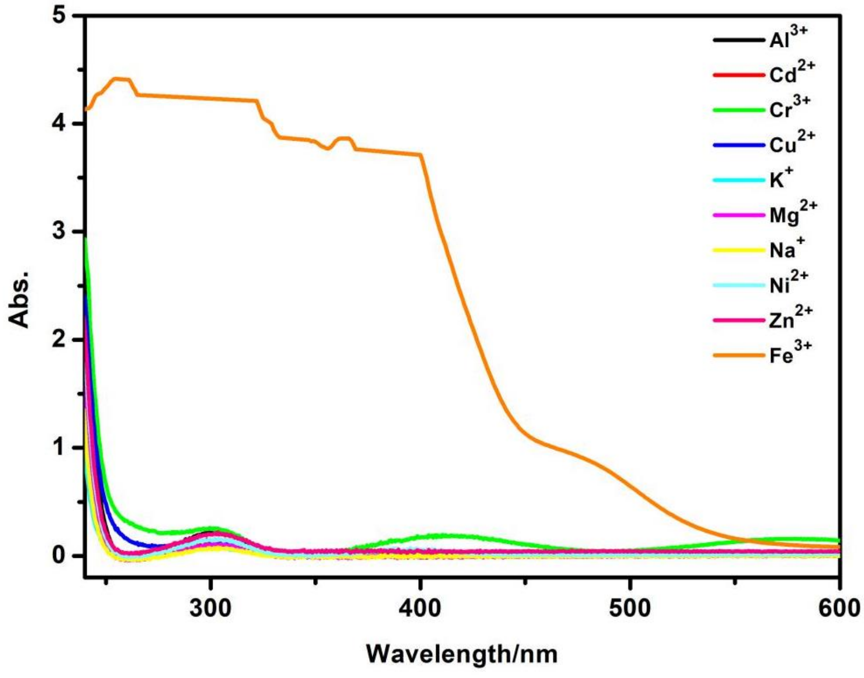

Figure **S14** Liquid UV/vis spectra of different metal cations in aqueous solutions.

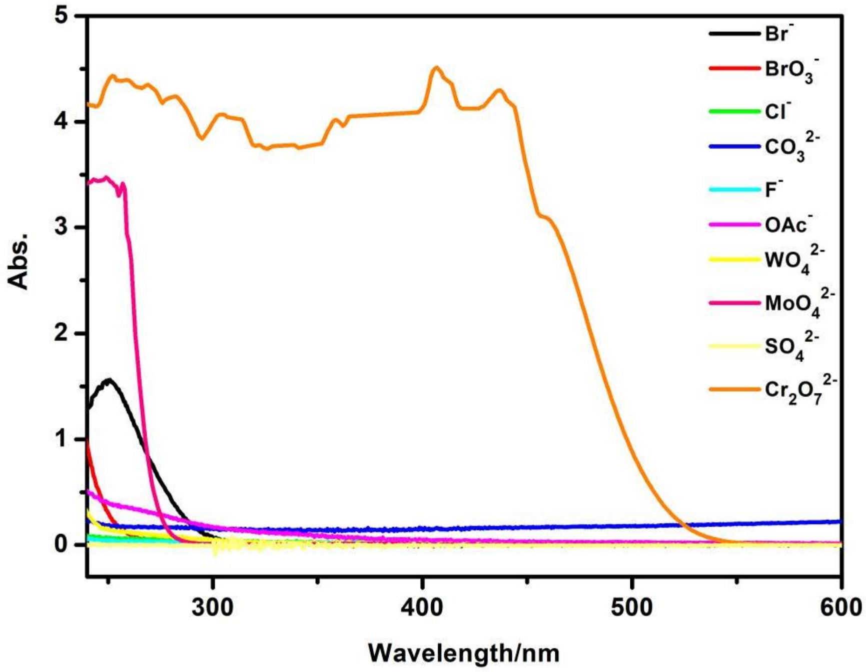

Figure **S15** Liquid UV/vis spectra of different anions in aqueous solutions.

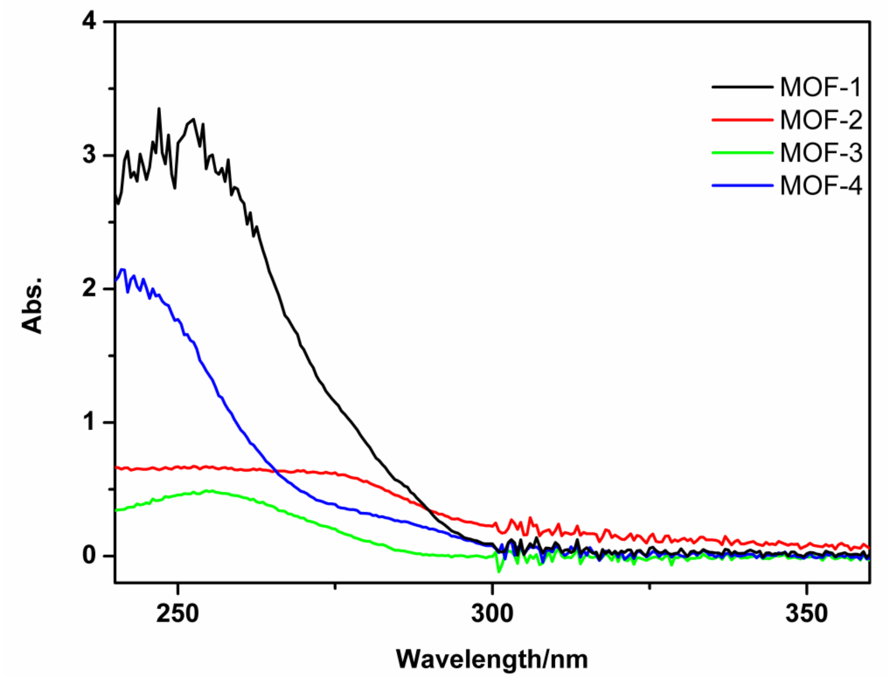

Figure **S16** Solid state UV/vis spectra of MOFs **1-4**.

Table **S1.** Crystal data and structure refinement for MOFs **1-4**.

MOFs	**1**	**2**	**3**[a]	**4**
Formula	$C_{32}H_{24}ZnN_2O_6S_3$	$C_{26}H_{20}ZnN_2O_4S_2$	$C_{32}H_{24}CdN_2O_5S_2$	$C_{32}H_{38}CdN_4O_8S_2$
Formula weight	694.08	553.93	693.05	783.18
Crystal system	Triclinic	Monoclinic	Triclinic	Triclinic
Space group	$P\bar{1}$	$C2/c$	$P\bar{1}$	$P\bar{1}$
a / Å	11.0591(19)	22.955(2)	9.5445(10)	7.2280(8)
b / Å	12.268(2)	6.2161(6)	12.8573(14)	10.7330(11)
c / Å	13.439(2)	19.744(2)	15.4179(17)	11.7457(13)
α / °	116.419(3)	90	106.726(2)	108.220(2)
β / °	94.590(3)	118.4960(10)	98.616(2)	91.311(2)
γ / °	102.601(3)	90	90.113(2)	100.104(2)
V / Å^3	1560.5(5)	2476.0(4)	1789.5(3)	849.15(16)
Z	2	4	2	1
D_{calcd} /g·cm^{-3}	1.477	1.486	1.286	1.532
μ / mm^{-1}	1.035	1.196	0.763	0.821
F(000)	712	1136	700	402
θ min-max / °	1.884, 27.473	2.019, 27.240	1.396, 27.160	1.832, 27.436
Tot., uniq. data	10643, 7093	10294, 2731	15596, 7757	5759, 3842
R(int)	0.0470	0.0369	0.036	0.0887
Observed data[I>2σ(I)]	7093	2731	7757	3842
N_{ref}, N_{par}	594, 490	0, 160	156, 418	225, 265
GOF on F^2	0.923	1.073	1.037	0.938
R_1, wR_2[I>2σ(I)][b]	0.0468, 0.1072	0.0348, 0.0920	0.0380, 0.1064	0.0415, 0.0902
R_1,wR_2 (all data)	0.0788, 0.1188	0.0407, 0.0974	0.0471, 0.1131	0.0510, 0.0938

[a] The residual electron densities were flattened by the SQUEEZE routine in PLATON.

[b] $R_1 = \Sigma||F_o|-|F_c||/\Sigma||F_o|$, $wR_2 = [\Sigma w(F_o^2-F_c^2)^2/\Sigma wF_o^4]^{1/2}$; where $w = 1/[\sigma^2(F_o^2)+(aP)^2+bP]$, $P = (F_o^2+2F_c^2)/3$.

Table **S2.** Selected bond lengths [Å] and angles [°] for MOFs **1-4**.

		1	
Zn(1)-O(4)#1	1.859(5)	Zn(1)-O(2)	2.121(2)
Zn(1)-N(1)	2.031(2)	Zn(1)-O(1)	2.254(2)
Zn(1)-N(2)	2.116(2)		
O(4)#1-Zn(1)-N(1)	127.2(3)	N(2)-Zn(1)-O(2)	97.63(9)
O(4)#1-Zn(1)-N(2)	90.9(2)	O(4)#1-Zn(1)-O(1)	98.6(2)
N(1)-Zn(1)-N(2)	100.09(9)	N(1)-Zn(1)-O(1)	90.93(9)
O(4)#1-Zn(1)-O(2)	127.3(3)	N(2)-Zn(1)-O(1)	156.86(10)
N(1)-Zn(1)-O(2)	102.40(9)	O(2)-Zn(1)-O(1)	59.92(8)
		2	
Zn(1)-O(1)#1	1.9384(16)	Zn(1)-N(1)#1	2.0505(19)
Zn(1)-O(1)	1.9384(16)	Zn(1)-N(1)	2.0505(19)
O(1)#1-Zn(1)-O(1)	100.81(11)	O(1)-Zn(1)-N(1)	124.28(8)
O(1)-Zn(1)-N(1)#1	104.13(8)	N(1)#1-Zn(1)-N(1)	101.41(11)
O(1)#1-Zn(1)-N(1)	104.13(8)	O(1)#1-Zn(1)-N(1)#1	124.28(8)
		3	
Cd(1)-O(2)	2.223(2)	Cd(1)-N(2)#3	2.372(2)
Cd(1)-O(1)#1	2.273(2)	Cd(1)-O(3)#2	2.391(2)
Cd(1)-N(1)	2.366(2)	Cd(1)-O(4)#2	2.366(2)
O(2)-Cd(1)-O(1)#1	102.35(9)	N(1)-Cd(1)-N(2)#3	166.56(11)
O(2)-Cd(1)-N(1)	104.81(10)	O(2)-Cd(1)-O(3)#2	150.02(9)
O(1)#1-Cd(1)-N(1)	90.60(9)	O(1)#1-Cd(1)-O(3)#2	105.39(9)
O(2)-Cd(1)-N(2)#3	88.27(10)	N(1)-Cd(1)-O(3)#2	86.14(10)
O(1)#1-Cd(1)-N(2)#3	83.46(8)	N(2)#3-Cd(1)-O(3)#2	83.84(9)

O(2)-Cd(1)-O(4)#2	96.51(9)	O(1)#1-Cd(1)-O(4)#2	160.00(9)
O(4)#2-Cd(1)-N(2)#3	90.58(9)	O(4)#2-Cd(1)-O(3)#2	54.85(9)
O(4)#2-Cd(1)-N(1)	90.97(9)		
		4	
Cd(1)-O(1)#1	2.281(2)	Cd(1)-N(1)	2.340(2)
Cd(1)-O(1)	2.281(2)	Cd(1)-O(1W)#1	2.356(3)
Cd(1)-N(1)#1	2.340(2)	Cd(1)-O(1W)	2.356(3)
O(1)#1-Cd(1)-O(1)	180.0	N(1)#1-Cd(1)-O(1W)#1	84.69(9)
O(1)#1-Cd(1)-N(1)#1	89.47(9)	N(1)-Cd(1)-O(1W)#1	95.31(9)
O(1)-Cd(1)-N(1)#1	90.53(9)	O(1)#1-Cd(1)-O(1W)	89.34(8)
O(1)#1-Cd(1)-N(1)	90.53(9)	O(1)-Cd(1)-O(1W)	90.66(8)
O(1)-Cd(1)-N(1)	89.47(9)	N(1)#1-Cd(1)-O(1W)	95.31(9)
N(1)#1-Cd(1)-N(1)	180.0	N(1)-Cd(1)-O(1W)	84.69(9)
O(1)#1-Cd(1)-O(1W)#1	90.65(8)	O(1W)#1-Cd(1)-O(1W)	180.00(9)
O(1)-Cd(1)-O(1W)#1	89.34(8)		

Symmetry codes: #1: *x*, *y*+1, *z*+1; #2: -*x*+3, -*y*+2, -*z*+2; #3: -*x*+1, -*y*, -*z*+1; #4: *x*, *y*-1, *z*-1 for **1**; #1: -*x*, *y*, -*z*+1/2; #2: -*x*+1/2, -*y*+3/2, -*z*+1; #3: -*x*, -*y*-1, -*z* for **2**; #1: -*x*+1, -*y*+2, -*z*+2; #2: *x*, *y*, *z*+1; #3: *x*-1, *y*+1, *z*; #4: *x*, *y*, *z*-1; #5: *x*+1, *y*-1, *z* for **3**; #1: -*x*+1, -*y*+1, -*z*+1; #2: -*x*, -*y*+2, -*z*+2; #3: -*x*+2,-*y*+2, -*z*+1 for **4**.